Biochimica et Biophysica Acta 1852 (2015) 1646–1657

Contents lists available at ScienceDirect

Biochimica et Biophysica Acta

journal homepage: www.elsevier.com/locate/bbadis

Sensitization to autoimmune hepatitis in group VIA calcium-independent phospholipase A2-null mice led to duodenal villous atrophy with apoptosis, goblet cell hyperplasia and leaked bile acids

Li Jiao [a,b], Hongying Gan-Schreier [a], Sabine Tuma-Kellner [a], Wolfgang Stremmel [a], Walee Chamulitrat [a,*]

[a] Department of Internal Medicine IV, University of Heidelberg Hospital, Heidelberg, Germany
[b] Department of Toxicology, School of Public Health, Jilin University, Changchun, China

ARTICLE INFO

Article history:
Received 9 January 2015
Received in revised form 27 April 2015
Accepted 28 April 2015
Available online 7 May 2015

Keywords:
Enterohepatic cycle
Pla2G6
Inflammation
Enteropathy
Hepatic necrosis
Bile acids

ABSTRACT

Chronic bowel disease can co-exist with severe autoimmune hepatitis (AIH) in an absence of primary sclerosing cholangitis. Genetic background may contribute to this overlap syndrome. We previously have shown that the deficiency of iPLA$_2$β causes an accumulation of hepatocyte apoptosis, and renders susceptibility for acute liver injury. We here tested whether AIH induction in iPLA$_2$β-null mice could result in intestinal injury, and whether bile acid metabolism was altered. Control wild-type (WT) and female iPLA$_2$β-null (iPLA$_2$β$^{-/-}$) mice were intravenously injected with 10 mg/kg concanavalinA (ConA) or saline for 24 h. ConA treatment of iPLA$_2$β$^{-/-}$ mice caused massive liver injury with increased liver enzymes, fibrosis, and necrosis. While not affecting WT mice, ConA treatment of iPLA$_2$β$^{-/-}$ mice caused severe duodenal villous atrophy concomitant with increased apoptosis, cell proliferation, globlet cell hyperplasia, and endotoxin leakage into portal vein indicating a disruption of intestinal barrier. With the greater extent than in WT mice, ConA treatment of iPLA$_2$β$^{-/-}$ mice increased jejunal expression of innate response cytokines CD14, TNF-α, IL-6, and SOCS3 as well as chemokines CCL2 and the CCL3 receptor CCR5. iPLA$_2$β deficiency in response to ConA-induced AIH caused a significant decrease in hepatic and biliary bile acids, and this was associated with suppression of hepatic Cyp7A1, Ntcp and ABCB11/Bsep and upregulation of intestinal FXR/FGF15 mRNA expression. The suppression of hepatic Ntcp expression together with the loss of intestinal barrier could account for the observed bile acid leakage into peripheral blood. Thus, enteropathy may result from acute AIH in a susceptible host such as iPLA$_2$β deficiency.

1. Introduction

The liver plays a major role in the defense against pathological insults and disease, such as, viral infection, metabolic syndrome, and autoimmune diseases, and thus this organ is prone to injury triggered by accumulated fat deposition and inflammatory cells. The injury to liver and bile ducts causes hepatobiliary autoimmune disease including primary biliary cirrhosis, primary sclerosing cholangitis (PSC), and autoimmune hepatitis (AIH), and this disease has an inherited element and clusters among families [1,2]. It is known that PSC is the most common hepatobiliary disease seen in association with inflammatory bowel disease (IBD), with 5% of all patients with IBD having PSC, and most patients with PSC ultimately develop IBD, usually chronic ulcerative colitis (UC) [2]. An overlap syndrome of PSC and AIH has also been seen in patients with UC, and severe AIH in an absence of PSC can lead to the development of UC with up to 16% of patients with AIH also having UC [3]. As patients with well-established AIH can develop PSC [4], and that those AIH patients with PSC in the background can develop progressive liver failure from AIH [5], this suggests that the common

Abbreviations: AB-PAS, alcian blue-periodic acid schiff; AIH, autoimmune hepatitis; ALT, alanine aminotransferase; AP, alkaline phosphatase; AST, aspartate aminotransferase; Bcl-2, B-cell lymphoma 2; CA, cholic acid; CCL, chemokine ligand; CCR, chemokine receptor; CDCA, chenodeoxycholic acid; CK19, cytokeratin 19; ConA, concanavalinA; CXCL12, C-X-C motif chemokine 12; DCA, deoxycholic acid; FXR, Farnesoid X-activated receptor; FGF15, fibroblast growth factor 15; H&E, hematoxylin-eosin; IHC, immunohistochemistry; iPLA$_2$β, group VIA calcium-independent iPLA$_2$; Klf4, Kruppel-like factor 4; LCA, lithocholic acid; LC-MS/MS, liquid-chromatography mass spectrometry; LDH, lactate dehydrogenase; LPA, lysophosphatidic acid; LPC, lysophosphatidylcholine; LPS, lipopolysaccharides; MCA, muricholic acid; MCP1, monocyte chemotactic protein1; PC, phosphatidylcholine; PPARγ, peroxisome proliferator activated receptorγ; PSC, primary sclerosing cholangitis; q-RT-PCR, quantitative real-time polymerase chain reaction; SHP, small heterodimer partner; SOCS3, suppressor of cytokine signaling 3; TNFα, tumor necrosis factorα; UDCA, ursodeoxycholic acid; VCAM1, vascular cell adhesion molecule 1; WT, wild-type; α-SMA, α-smooth muscle actin

* Corresponding author at: Internal Medicine IV, Im Neuenheimer Feld 345 EG, 69120 Heidelberg, Germany. Tel.: +49 6221 5638731; fax: +49 6221 565398.
E-mail address: Walee.Chamulitrat@med.uni-heidelberg.de (W. Chamulitrat).

http://dx.doi.org/10.1016/j.bbadis.2015.04.025
0925-4439/

mechanism of AIH and PSC overlap syndrome for UC and IBD may involve a cholestatic phenotype with cholangiopathy and histologic changes of bile duct injury [3,6] as well as alteration in bile acids within the enterohepatic system [7]. Intestinal inflammation and injury has been reported in experimental cirrhosis [8], as well as in patients with decompensated [9] and alcoholic [10] cirrhosis, and the latter has been shown to be associated with alteration in bile acid metabolism. No experimental data have ever been presented to report the involvement of AIH in IBD to confirm patient studies [3], and whether the mechanism is genetically dependent.

In defining a pathogenic mechanism for a contribution of AIH to bowel disease, we designed a mouse AIH model by using a combination of concanavalin A (ConA) [11], and a genetically susceptible transgenic mouse model [12]. ConA induces hepatitis in mice is by an activation of T cells and macrophages with massive granulocyte and CD4 T cell infiltration which leads to apoptosis and necrosis in the hepatocytes and biliary epithelial cells. The latter corresponds to the cholestatic phenotype which is regulated by bile acids [13,14]. Hence, AIH pathogenesis may involve alteration in bile acid metabolism in the enterohepatic loop [10,14] that may play a pivotal role in intestinal homeostasis leading to bowel injury and disease [8–10].

In evaluating a genetically susceptible mouse model, we chose group VIA calcium-independent phospholipase A2 (iPLA$_2$) with alterative names of Pla2G6 or iPLA$_2\beta$ [15], because it has multiple physiologically important functions in numerous cell types and tissues [16]. iPLA$_2\beta$ catalyzes phospholipids to generate 1). lysophosphatidylcholine (LPC) which acts as a 'find-me' signal for removal of apoptotic cells by monocytes [17,18], and 2). lysophosphatidic acid (LPA) plays a role in the migration of monocytes [19,20], and of ovarian cancer cells [21]. Despite of the anticipated dysfunction with iPLA$_2\beta$ deficiency, iPLA$_2\beta$-null mice with the deletion of the lipase-containing exon 9 live normally, but they have defects in glucose homeostasis [15], gain lesser body weight [22], and develop neuroaxonal dystrophy [23] as they age to 1–2 years old. In line with a decrease of LPC leading to a defect in the removal of apoptotic hepatocytes, results from our laboratory have shown that hepatic apoptosis was indeed increased in the livers of iPLA$_2\beta$-null mice together with increased inflammation and susceptibility for endotoxin injury [24] (manuscript under preparation). Because apoptosis is the predominant mechanism of liver cell death during AIH [25], we hypothesize that the deficiency of iPLA$_2\beta$ would represent a genetic susceptible preconditioning for AIH that could lead to bowel injury.

Here we compared the extent of AIH liver injury induced by ConA between wild-type (WT) and iPLA$_2\beta$-null (iPLA$_2\beta^{-/-}$) mice, and determined whether AIH observed in liver was associated with abnormalities in the intestine and colon in regards to epithelial damage, proliferation and bile acid contents. We demonstrated that iPLA$_2\beta$ deficiency sensitized the effects of ConA in promoting liver injury as well as duodenal apoptosis, villous atrophy, intestinal inflammation, goblet cell hyperplasia, and leakage of endotoxin into portal vein. Alteration of bile acids was observed in liver, bile, intestine, feces, and peripheral blood during ConA and iPLA$_2\beta$-deficiency sensitization. Gene expression analysis revealed a feedback regulation of hepatic bile acid synthesis by intestinal FXR/FGF15 axis. Thus, ConA-induced AIH in a susceptible host with iPLA$_2\beta$ deficiency led to enteropathy which was associated with alteration in bile acid metabolism. Our data support the notion that the liver-to-gut axis injury due to AIH in susceptible individuals may lead to bowel disease.

2. Materials and methods

2.1. Animals and treatment

iPLA$_2\beta^{-/-}$ mice were kind gifts from Dr. John Turk (Washington University School of Medicine, St. Louis, Missouri, USA). The breeding and genotyping was performed according to the published work [15]. Control WT mice were mice with iPLA$_2\beta^{+/+}$ phenotype. All mice were housed at the animal facility of the University Heidelberg. Female mice at 13–16 months old were used. For an AIH induction, mice were intravenously injected via tail vein with 10 mg/kg Con A (Sigma Aldrich, Taufkirchen, Germany) or saline. Blood, liver, bile, intestine, colon, and feces were harvested 24 h after ConA administration. All animal experiments were approved by the Animal Care and Use Committee of the University of Heidelberg.

2.2. Biochemical assays

Serum was obtained after centrifugation at 5000 *g* for 15 min. Serum activities of alanine aminotransferase (AST), aspartate aminotransferase (AST), lactate dehydrogenase (LDH), and alkaline phosphatase (AP) were measured spectrophotometrically by using diagnostic kits from Randox (Krefeld, Germany).

2.3. Histology and immunohistochemistry (IHC)

Liver, intestine and colon specimens were fixed in 10% formalin at room temperature for 18 h, and embedded in paraffin, and paraffin blocks were cut into 5 μm sections. Sections were stained with hematoxylin and eosin (H&E) for histology. For Sirius-red staining of the liver, sections were stained with 0.1% Direct Red 80 Solution (Sigma Aldrich) in a saturated solution of picric acid. For mucin staining of intestine, slides were stained with alcian blue-periodic acid schiff (AB-PAS) reagents (Sigma Aldrich) according to standard procedure.

For IHC, after deparaffinizing and hydration, sections were treated with 10 mM citrate buffer (pH 6.0) and heated to 98 °C for 20 min. Endogenous peroxidase was blocked by treating sections with 3% H_2O_2 for 10 min at room temperature prior to an exposure to a primary antibody overnight at 4 °C. Rabbit primary antibodies used for IHC were cleaved caspase-3 (1:800; cat# 9664, Cell Signaling), α-SMA (1:250; E184, Epitomics), CK19 (1:100; cat# ab133496, Abcam), Ki67 (1:100; cat# ab16667, Abcam), CD3 (1:300; cat# ab5690, Abcam), and CD45R (1:200; cat# ab64100, Abcam). Sections for cleaved caspase-3 staining were stained by using an Abcam Avidin-Biotin Complex kit (cat# ab64261), and the rest of antibodies sections were incubated with a goat anti-rabbit secondary Abcam antibody (cat# ab6721) for 1 h at room temperature. Positive staining was detected by diaminobenzidine. Slides were counterstained with hematoxylin prior to mounting.

Light microscopy was used to visualize stained cells with an Olympus IX 50 microscope. The quantification of Sirius-red- and α-SMA-positive areas in liver was performed by using Image J. For computerized image analyses of intestine, the number of stained cells on a surface area of epithelial cells were determined by using the Olympus Cell^F software. A picture of one field on a slide taken with a 20X objective corresponded to 0.6 mm^2 on the tissue. The number of stained cells on each slide was counted from ten randomly selected fields. Data were presented as the number of stained cells per mm^2 of intestinal epithelium. Evaluation of IHC sections was performed in a blind manner.

2.4. Bile acid profiling using LC-MS/MS

Samples were subjected to extraction using a published method [26], and bile acid concentrations were determined by using liquid-chromatography mass spectrometry (LC-MS/MS) according to a published method [27]. Briefly, the separation of bile acids was achieved by using a Phenomenex Luna C18 column (100 mm × 2.0 mm, 3 μm) fitted on a separation module of a Waters 2695. Binary solvents were 80% H_2O/MeOH with 8 mM ammonium acetate, pH 8.0 (solvent A) and 95% MeOH/H_2O with 8 mM ammonium acetate, pH 8.0 (solvent B). The flow rate was maintained at 0.2 mL/min, and the gradient was started with 100% solvent A for 2.5 min, changed to 100% solvent B in 1 min, held for 16.5 min, and returned to the initial condition in 3 min. Separated fractions were detected on-line by an electrospray

ionization source of the tandem mass spectrometer (Quattro micro API, Micromass Waters).

2.5. Gene expression analyses

Total RNA was isolated by using the QIAGEN RNeasy Mini kit (Qiagen, Hilden, Germany). cDNA was synthesized from 2 μg RNA by using a Maxima First Strand cDNA synthesis kit (Fermentas, St. Leon-Rot, Germany). Gene expression was analyzed by quantitative real-time polymerase chain reaction (q-RT-PCR) using Applied Biosystems TaqMan® gene expression assays with TaqMan® Universal PCR Master Mix, and run on an Applied Biosystem 7500. The expression level of targets in quadruplets was calculated using the Δ–C_t transformation method, and determined as a ratio of the target gene normalized to the house-keeping gene GAPDH.

2.6. Western blot analyses

Tissue homogenates were obtained after centrifugation at 13,000 *g* at 4 °C for 15 min, and proteins were determined by using Bio-Rad protein^{DC} kit (Bio-Rad laboratories, Munich, Germany). Proteins were separated by gel electrophoresis and transferred onto a PDVF membrane. Blots were probed with a primary antibody at 1:1000 dilution overnight at 4 °C followed by a secondary antibody. Primary antibodies used for Western blot included a rabbit antibody against iPLA$_2\beta$ (cat # sc-14463, Santa Cruz), cleaved caspase 3 (cat# 9664, Cell Signaling), CCL2 (cat #2027, Cell Signaling), and PPARγ (cat #2435, Cell Signaling). Proteins were visualized using the Luminata Forte ECL reagent (Millipore, Darmstadt, Germany). Image J was used to quantify the density of protein bands of the targets and loading control GAPDH, and the ratio of protein target/GADPH was calculated.

2.7. Measurement of LPS in mouse serum

The concentrations of LPS in mouse portal vein serum were determined by using Mouse Lipopolysaccharides (LPS) ELISA Kit cat # MBS040441 (Biozol GmbH, Eching, Germany) according to manufacturer's instructions. In brief, 50 μl serum and HRP-conjugated reagent were added into a pyrogen-free microplate well. After 60-min incubation at 37 °C, the sample mixture was added with 100 μl of substrate solution followed by an addition of 50 μl stop buffer after 16-min incubation. The absorbance was then measured at 450 nm.

2.8. Statistics

Results were expressed as mean ± SEM. Significance was accepted at $p < 0.05$. For lipidomics data, statistical significance for multiple comparisons was computed using the R multcomp for multiple comparisons of all pairwise differences of mean (Tukey contrasts). For the rest of the data, significance using ANOVA with Turkey's post hoc test for multiple comparisons was determined by using GraphPad Prism 5.

3. Results

3.1. iPLA$_2\beta$ deficiency increases susceptibility towards ConA-induced liver injury

We have previously found that iPLA$_2\beta^{-/-}$ mice were susceptible for endotoxin liver injury [24] (manuscript under preparation), we therefore determined whether this would be the case for ConA-induced AIH. With a low dose of ConA (10 mg/kg) injected for 24 h, ConA nearly had no effects on activities of liver enzymes (ALT, AST, LDH and AP) in control WT mice, while marked elevation of these activities was observed in iPLA$_2\beta^{-/-}$ mice (Fig. 1A). This increased liver injury was consistent with histological changes seen in H&E stained liver sections (Fig. 1B). ConA-treated WT livers showed minimal pathological abnormalities while ConA-treated mutant livers showed macroscopic lesions with necrotic areas (marked with N) and a wider sinusoid space (Fig. 1B). ConA treatment established an AIH as seen by the presence of recruited lymphocytes stained with CD3 T cell and CD45R B cell markers, and the extent of lymphocyte infiltration was greater in iPLA$_2\beta^{-/-}$ knockout mice (Fig. 1C).

AIH causes liver inflammation and is commonly associated with progressive fibrosis. We consistently observed that the livers of iPLA$_2\beta^{-/-}$ mice showed increased collagen deposition seen by Sirius-red staining (Fig. 1D) as well as activation of hepatic stellate cells seen by α-SMA IHC (Fig. 1E). Quantification of both fibrosis markers represented as % positive area showed that ConA treatment induced fibrosis in both WT and mutant mice, but with a greater extent in mutant than in WT mice.

To further investigate the mechanism of iPLA$_2\beta$ in ConA-induced AIH, we analyzed cell proliferation by assessing an S phase maker Ki67 in livers. We found that IHC staining of Ki67 was positive on the lymphocytes in livers of saline- and ConA-treated iPLA$_2\beta^{-/-}$ mice, and the latter with increased lymphocyte infiltration with many more cells showing positive for Ki67 (Fig. 1F). Proliferative lymphocytes were seen surrounding the portal tract in mutant livers indicating moderate inflammation by iPLA$_2\beta$ deficiency alone, and in response to ConA massive lymphocyte infiltration was seen around portal tract and nearby adjacent parenchyma. At the portal tract, ConA-induced lymphocytes may induce an activation of ductular reaction of the bile ducts resulting in a cholestatic phenotype [13]. By IHC staining of cytokeratin 19 (CK19), a marker of biliary epithelial cells, we consistently observed moderately increased CK19 staining in iPLA$_2\beta^{-/-}$ livers when compared with WT livers (Fig. 1G). Marked increased CK19 staining was observed in livers of ConA-treated mutant mice with a greater extent than those of WT mice. These findings indicated that iPLA$_2\beta$ was critical in the homeostasis of hepatobiliary system, and that its deficiency rendered susceptibility for ConA-induced injury in the hepatocytes and biliary epithelial cells. Hence, iPLA$_2\beta^{-/-}$ mice undergoing AIH were a suitable model system for further investigation on abnormalities in the intestine and alteration in bile acid profiles.

3.2. Lack of iPLA$_2\beta$ disrupts intestinal integrity associated with increased apoptosis

The genetic deletion of exon 9 in iPLA$_2\beta$ gene led to a complete absence of iPLA$_2\beta$ protein detectable at 85 KDa and mRNA expression in the duodenum of iPLA$_2\beta^{-/-}$ compared with that of WT mice (Fig. 2A). Interestingly, ConA treatment slightly increased expression of iPLA$_2\beta$ protein in the mutant intestine suggesting a feedback regulation of iPLA$_2\beta$ presumably necessary for the proliferation of lymphocytes triggered by ConA [28]. Histological analysis showed that ConA treatment nearly had no effects in WT duodenum, but caused severe damage in mutant intestinal epithelial cells associated with exposed lamina propria, shorter villi, disturbed mucus membrane, and mucosal atrophy (Fig. 2B). We hypothesize that deficiency of iPLA$_2\beta$ producing a decrease in the 'find-me-signal' LPC could result in an accumulation of apoptotic cells in intestine. Compared with WT duodenum, we consistently observed an increase in apoptosis in mutant duodenum as seen by IHC (marked with black arrow heads) and Western blot analysis of cleaved caspase 3 (Fig. 2C). In a greater extent in the mutant than in the WT duodenum, ConA treatment further increased the shedding of apoptotic epithelial cells as seen by cleaved caspase 3 IHC showing positive staining towards the top of the villi. This sensitization to ConA was not due to changes in anti-apoptosis proteins, since we observed no difference in duodenal mRNA expression of anti-apoptosis TNFAIP3 and Bcl2 in ConA-treated WT and ConA-treated mutant mice (Supplementary Fig. S1).

As we previously observed increased proliferative lymphocytes in livers of ConA-treated mutant mice (Fig. 1C and F), we further evaluated the extent of cell proliferation in the intestine. ConA treatment of mutant mice increased the number of Ki67 (+) cells in the duodenal crypts

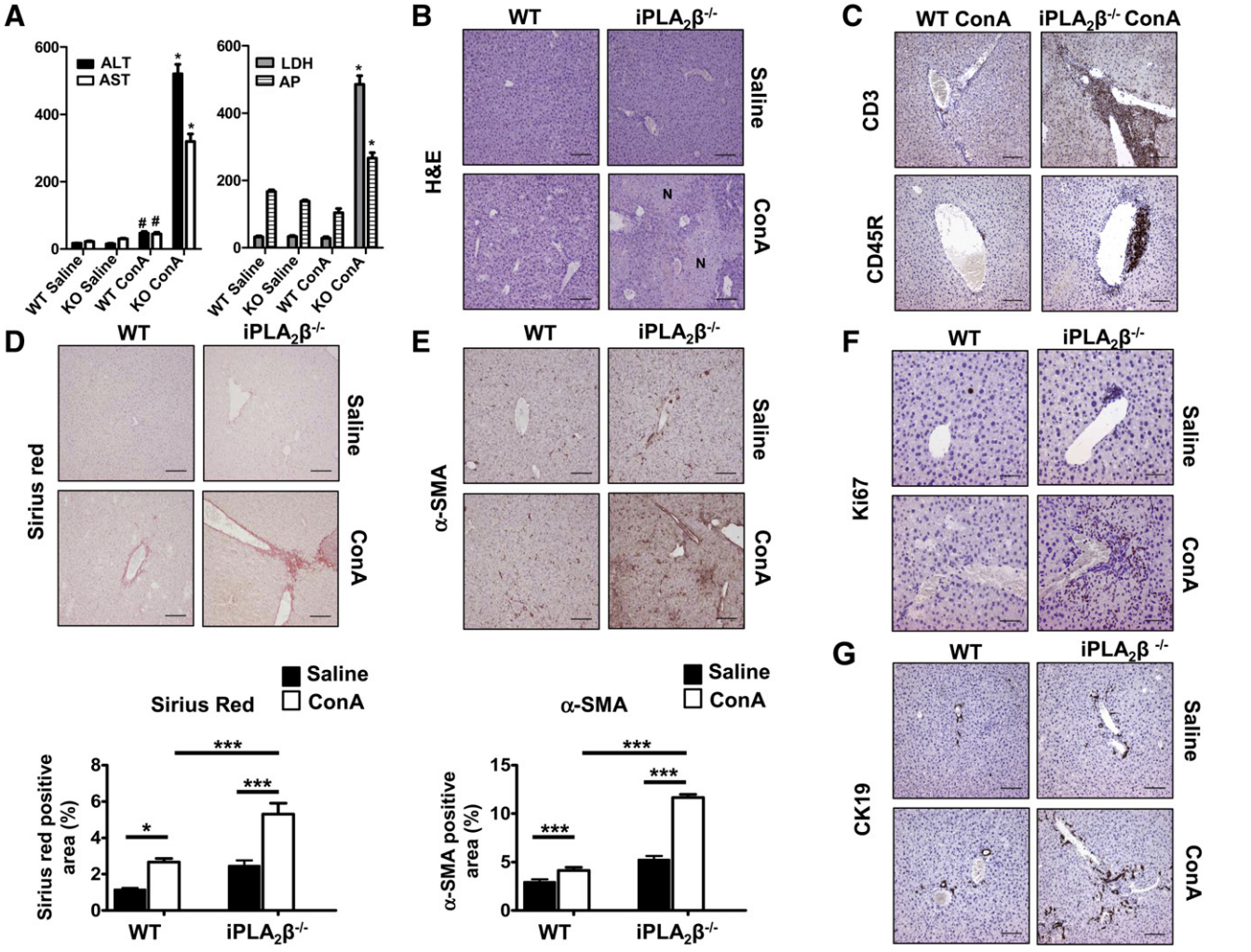

Fig. 1. Hypersensitivity towards ConA-induced autoimmune hepatitis by iPLA$_2$β deficiency. WT and iPLA$_2$β$^{-/-}$ mice were intravenously injected with 10 mg/kg ConA or saline for 24 h. Our experimental system comprised of 4 groups: ConA-treated iPLA$_2$β$^{-/-}$, ConA-treated WT, saline-treated iPLA$_2$β$^{-/-}$, and saline-treated WT mice. A. ALT, AST, LDH and AP activities in serum samples of treated mice from four groups. Data are mean ± SEM (N = 6–8): ***, $p < 0.001$ vs WT. B. Representative H&E staining of the livers of treated mice from four groups. N indicates necrosis area. C. CD3 and CD45R IHC staining of the livers of ConA-treated WT or iPLA$_2$β$^{-/-}$ mice. D. Sirius-red staining of the livers (upper panel) and its quantification (lower panel) of treated mice from four groups. Data are mean ± SEM (N = 3–4); *, $p < 0.05$; ***, $p < 0.001$. E. α-SMA IHC staining of the livers (upper panel) and its quantification (lower panel) of treated mice from four groups. Data are mean ± SEM (N = 3–4); ***, $p < 0.001$. F. Ki67 IHC staining of the livers of treated mice from four groups. G. CK19 IHC staining of the livers of treated mice from four groups. Scale bar in histological pictures represents 200 μm.

(Fig. 2D) and colonic crypts (Fig. 2E) to a greater extent than that of WT mice. This observation likely revealed a simultaneous activation of the regeneration of enterocytes and colonocytes in order to compensate for epithelial cell loss due to ConA-induced villous damage. Notably, compared with WT mice it was also observed that the colon of mutant mice already had an elevated number of Ki67 (+) cells which was not further increased by ConA (Fig. 2E), emphasizing an inherent effect of iPLA$_2$β deficiency on colonic proliferation. This lack of ConA effect in the mutant colon may indicate an anatomical distance away from the liver as to compare with the effect observed in the mutant duodenum.

3.3. Effects of iPLA$_2$β deficiency on ConA-induced inflammatory response in the intestine

In an association with increased duodenal apoptosis and atrophy (Fig. 2B), we further determined whether ConA combined with iPLA$_2$β deficiency increased an inflammatory response by qRT-PCR analyses. ConA treatment of mutant mice caused and induction of innate immune response as seen by an increase in jejunal mRNA expression of an innate response receptor CD14, TNF-α, IL-6, and suppressor of cytokine signaling 3 (SOCS3) when compared with Con-treated WT mice (Fig. 3A). ConA treatment however increased IL-10 and IL-1β mRNA expression to the same extent in both WT and mutant mice (Supplementary Fig. S2A). As chemokines contribute to the pathogenesis of AIH by directing the migration and positioning of inflammatory and immune cells, we analyzed jejunal expression of various chemokines. The involvement of CCL3/CCR5 axis in ConA-induced inflammatory response was observed in mutant jejunum with a tendency and a significant increase of CCL3 and CCR5, respectively (Fig. 3B). Among other chemokines including CXCL12, VCAM1, CCR1, CCL4, and CCL5, ConA treatment increased expression of these chemokines to the same extent among WT and mutant mice (Fig. 3B, and Supplementary Fig. S2B). No ConA response was observed among WT and mutant intestine for lymphocyte markers CD4, CD8, endothelial cell marker CD34, as well as dendritic cell marker CD11b, CD11c, and F480 (Supplementary Fig. S2 C). Unlike the observation in the liver (Fig. 1F), ConA treatment appeared not to sensitize the infiltration of lymphocytes and immune cells to the mutant intestine suggesting that ConA primarily induced the innate immune response in this organ in an iPLA2β-dependent manner.

The most affected chemokine was CC chemokine ligand 2 (CCL2) or monocyte chemoattractant protein1 (MCP1) as seen by an increased expression of CCL2 protein and mRNA in the jejunum of ConA-treated mutant mice when compared with that in ConA-treated WT mice

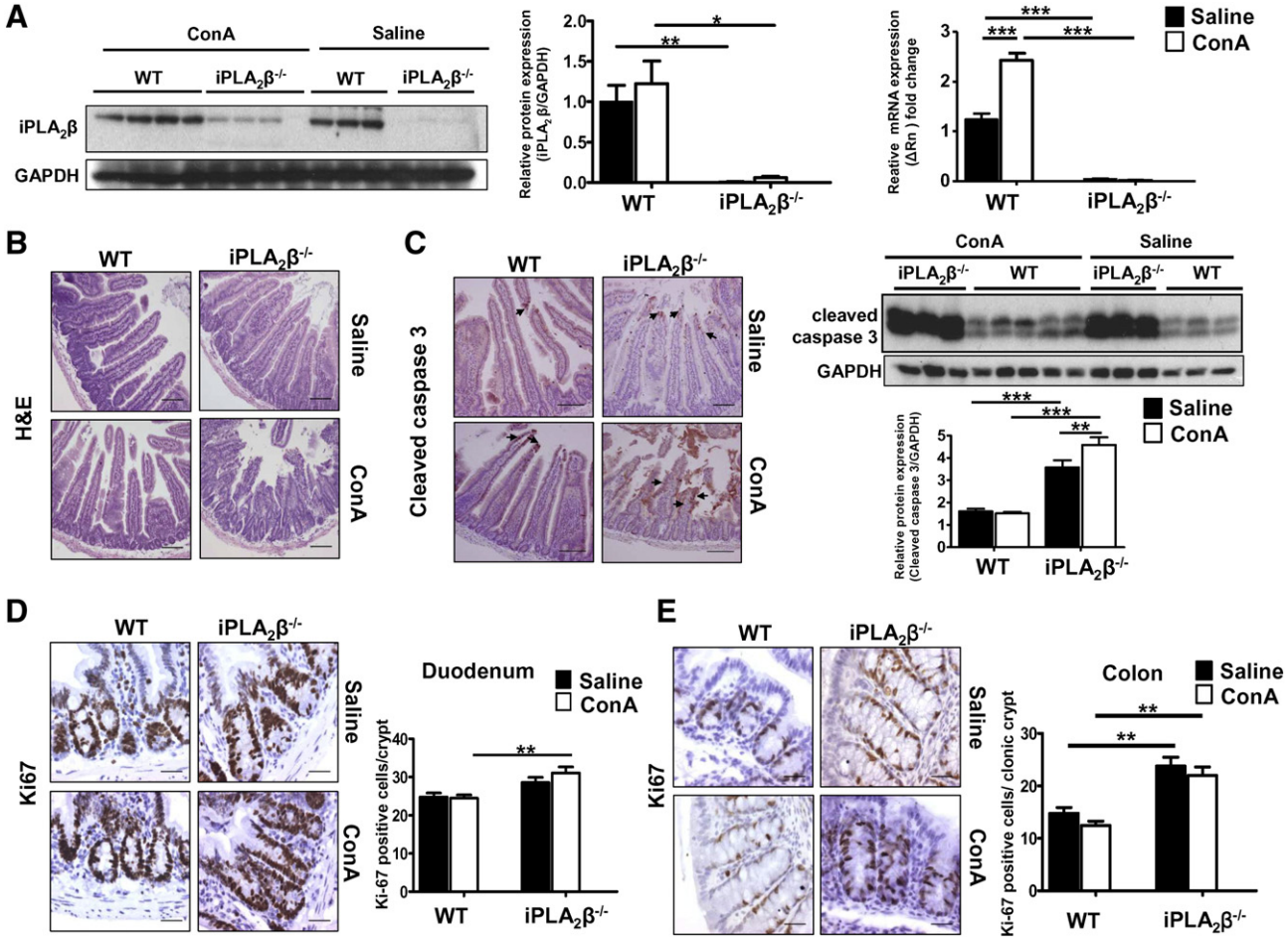

Fig. 2. Lack of iPLA$_2$β causes duodenal villous atrophy by increasing apoptosis. Experimental conditions were the same as described in Fig. 1. A. Western blot analyses (left), protein quantification (middle) and qRT-PCR analysis (right) for iPLA$_2$β expression in the duodenum of treated mice from four groups. Data are mean ± SEM (N = 3–8); *, $p < 0.05$; **, $p < 0.01$; ***, $p < 0.001$. B. Representative histological images from H&E-stained duodenal sections from treated mice from four groups. C. Cleaved caspase 3 IHC staining (left), Western blot analyses (right, upper panel), protein quantification (right, lower panel) in the duodenum of treated mice from four groups. Data are mean ± SEM (N = 3–5); **, $p < 0.01$; ***, $p < 0.001$. D. Representative Ki67 staining of the duodenal crypts of treated mice from four groups. Data are mean ± SEM (N = 4); **, $p < 0.01$. E. Representative Ki67 staining of the colonic crypts of treated mice from four groups. Data are mean ± SEM (N = 4); **, $p < 0.01$. Scale bar in histological pictures represents 200 μm.

(Fig. 3C). However, ConA treatment increased jejunal mRNA expression of the CCL2 receptor CCR2 to the same extent in WT and mutant mice. As we observed that immune cell infiltration to the intestine was not involved during ConA and iPLA$_2$β deficiency sensitization (Supplementary Fig. S2B), we interpret these results that the increased jejunal MCP1 would unlikely be derived from activity of immune cells, but rather from the accumulated apoptotic intestinal epithelial cells themselves in order to attract phagocytes for their effective removal.

iPLA$_2$β catalyzes phosphatidic acid to LPA which has been shown to mediate cell migration [19–21]. To delineate possible role of iPLA$_2$β-derived LPA during ConA and iPLA$_2$β-deficiency sensitization, we analyzed the expression of an intracellular receptor LPA peroxisome proliferator activated receptorγ (PPARγ) [29]. ConA treatment of iPLA$_2$β$^{-/-}$ mice caused a significant decrease in jejunal protein and mRNA expression of PPARγ, while no effect was observed in ConA-treated WT mice (Fig. 3D). We further determined expression of class B scavenger receptor CD36 which is under the transcriptional control of PPARγ [30], and CD36 has been shown to play a role in mediating the recognition and elimination of apoptotic cells [31]. Consistently, CD36 mRNA expression was significantly decreased in the jejunum of ConA-treated mutants when compared with that of ConA-treated WT mice (Fig. 3D). Thus, ConA and iPLA$_2$β-deficiency sensitization in intestine was likely associated with accumulated apoptosis due the defects in 'fine-me' signal LPC as well as the defects in LPA-activation of PPARγ and CD36.

3.4. iPLA$_2$β-deficient mice treated with ConA exhibit severely disturbed mucus membrane, duodenal goblet cell hyperplasia, and endotoxin leakage into portal vein

Intestinal goblet cells secrete mucins to form a mucus layer as a host-defense barrier against variety of enteric pathogens, and inflammation of mucous membrane can contribute to the development of diarrhea. To determine whether there was dysfunction in goblet cell-mediated mucin secretion during ConA-induced intestinal injury in mutants, we stained acidic and neutral mucins in the duodenum, ileum, and colon by using alcian blue-periodic acid schiff (AB-PAS) reagents. We observed AB-PAS blue stains on the mucus membrane layer on the luminal side of intestine (indicated by red arrows) and on the goblet cells (Fig. 4). Compared with saline treatment, ConA treatment of mutant mice increased the number of mucin-containing globlet cells in all the tissues examined (Fig. 4A–C). In the duodenum of ConA-treated mutant mice, there was an increase of blue-stained mucins on the mucus membrane and on the goblet cells, and the latter was shown with an increase of the number of mucin-containing globlet cells when compared with that of ConA-treated WT mice (Fig. 4A). This increase was suggestive of either an active mucin secretion or new synthesis of mucins, or both, during ConA and iPLA$_2$β-deficiency sensitization. In the ileum of ConA-treated mutant mice, an increase of number of mucin-containing globlet cells was also observed while no disruption of mucus membrane was observed (Fig. 4B). Finally, no changes in

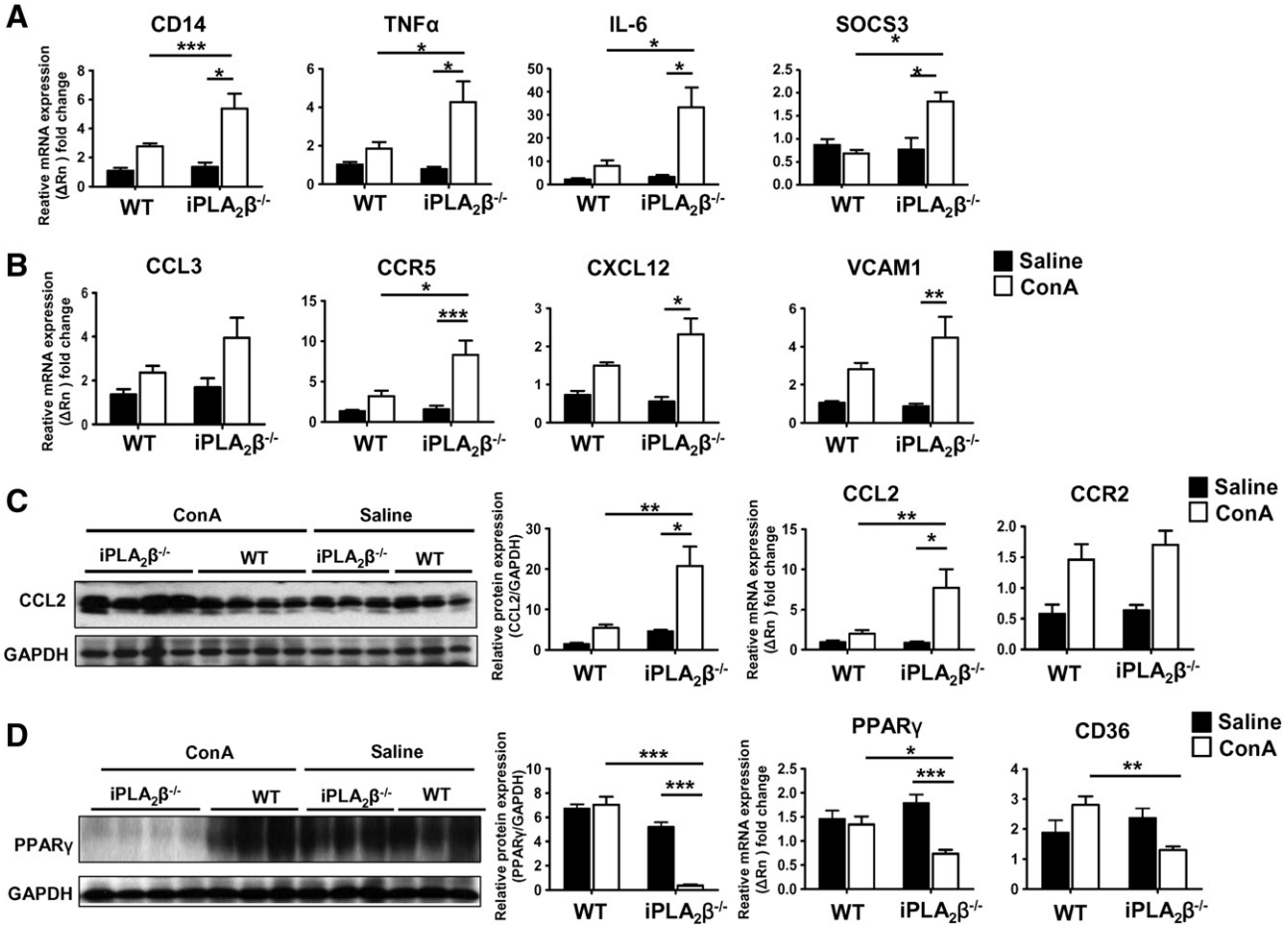

Fig. 3. iPLA$_2$β deficiency sensitizes ConA-induced inflammatory response in the intestine. Experimental conditions were the same as described in Fig. 1. A. qRT-PCR analysis of CD14, TNFα, IL-6 and SOCS3 mRNA expression in the jejunum of treated mice from four groups. Data are mean ± SEM (N = 6–8); *, $p < 0.05$; ***, $p < 0.001$. B. qRT-PCR analysis of CCL3, CCR5, CXCL12, and VCAM1 mRNA expression in the jejunum of treated mice from four groups. Data are mean ± SEM (N = 6–8); *, $p < 0.05$; ***, $p < 0.001$. C. Western blot analyses normalized with GADPH (left), qRT-PCR analysis (middle) of CCL2 expression, and qRT-PCR analysis of CCR2 expression (right) in the jejunum of treated mice from four groups. Data are mean ± SEM (N = 3–8); *, $p < 0.05$; **, $p < 0.01$. D. Western blot analyses normalized with GADPH (left), qRT-PCR analysis (middle) of PPARγ expression, and qRT-PCR analysis of CD36 expression (right) in the jejunum of treated mice from four groups. Data are mean ± SEM (N = 3–8); *, $p < 0.05$; **, $p < 0.01$; ***, $p < 0.001$.

mucus layer and in the number of mucin-containing globlet cells were observed in the colon of WT and mutant mice treated with ConA (Fig. 4C). These results showed the presence of disrupted mucus membrane and goblet cell hyperplasia in the duodenum, and the severity became lesser in the distal intestine and colon. Thus, the duodenum was the most affected because of its closer proximity to the liver where AIH sensitization was initiated.

To elucidate the mechanism responsible for goblet cell hyperplasia in the intestine of ConA-treated iPLA$_2\beta^{-/-}$ mice, we analyzed two key target genes shown to regulate the differentiation of globlet cells, namely, Kruppel-like factor 4 (Klf4) and cyclin D2. Klf4 is a zinc finger transcription factor required for intestinal goblet cell differentiation [32]. Here, we found that ConA treatment of mutant mice increased intestinal Klf4 mRNA expression to a greater extent than that of WT mice (Fig. 4D). Cyclin D2 is an inhibitor of cyclin-dependent kinases whose activity is required for cell cycle G1/S transition, and the transcriptional upregulation of cyclin D2 has been shown to protect mice from developing intestinal goblet cell metaplasia [33]. ConA treatment of WT mice induced a marked upregulation of intestinal cyclin D2 (Ccnd2) mRNA, but failing to so in iPLA$_2\beta^{-/-}$ mice (Fig. 4E). The observed defect in Ccnd2 activation in the mutants by ConA was consistent with the increased goblet cell hyperplasia (Fig. 4 A), and also the observed increases of Ki67 (+) proliferation in intestinal crypts (Fig. 2D). Hence, our results showed that ConA and iPLA$_2\beta$-deficiency sensitization induced intestinal goblet cell hyperplasia by a mechanism involving goblet cell differentiation at least in part mediated by Klf4 and cyclin D2.

The observed disruption of duodenal mucus membrane during ConA and iPLA$_2\beta$-deficiency sensitization shown in Fig. 4A would allow a leakage of luminal bacteria into intestine and entering into portal vein. Consistently, LPS levels in the portal vein serum obtained from ConA-treated iPLA$_2\beta^{-/-}$ mice were increased compared with those in the serum obtained from ConA-treated WT mice (Fig. 4F). These effects were not statistically significant for serum LPS obtained from peripheral blood (data not shown).

3.5. iPLA$_2\beta$ deficiency alone and in response to ConA causes alteration in bile acid metabolism and transport in liver and intestine

To this end, iPLA$_2\beta$ deficiency sensitized the effects of ConA increasing the injury on the hepatocytes and biliary epithelial cells with necrosis, fibrosis and ductular reaction (Fig. 1), and this was associated with intestinal apoptosis (Fig. 2), inflammation (Fig. 3), and goblet cell hyperplasia (Fig. 4) with the most effects observed in the duodenum. Since bile is secreted from liver into duodenal lumen, we further investigated whether these abnormalities would be associated with alteration in bile acid metabolism. Bile acids are synthesized from cholesterol by Cyp7A1 in the liver into primary bile acids: cholic acid (CA), muricholic acid (muriCA), chenodeoxycholic acid (CDCA), which is conjugated with glycine and taurine amino acids to form glyco- and tauro-bile acids. After bile acid secretion into gut lumen, gut bacteria perform deconjugation and dehydroxylation to produce secondary bile acids deoxycholic acid (DCA), lithocholic acid (LCA), and 7-oxo-

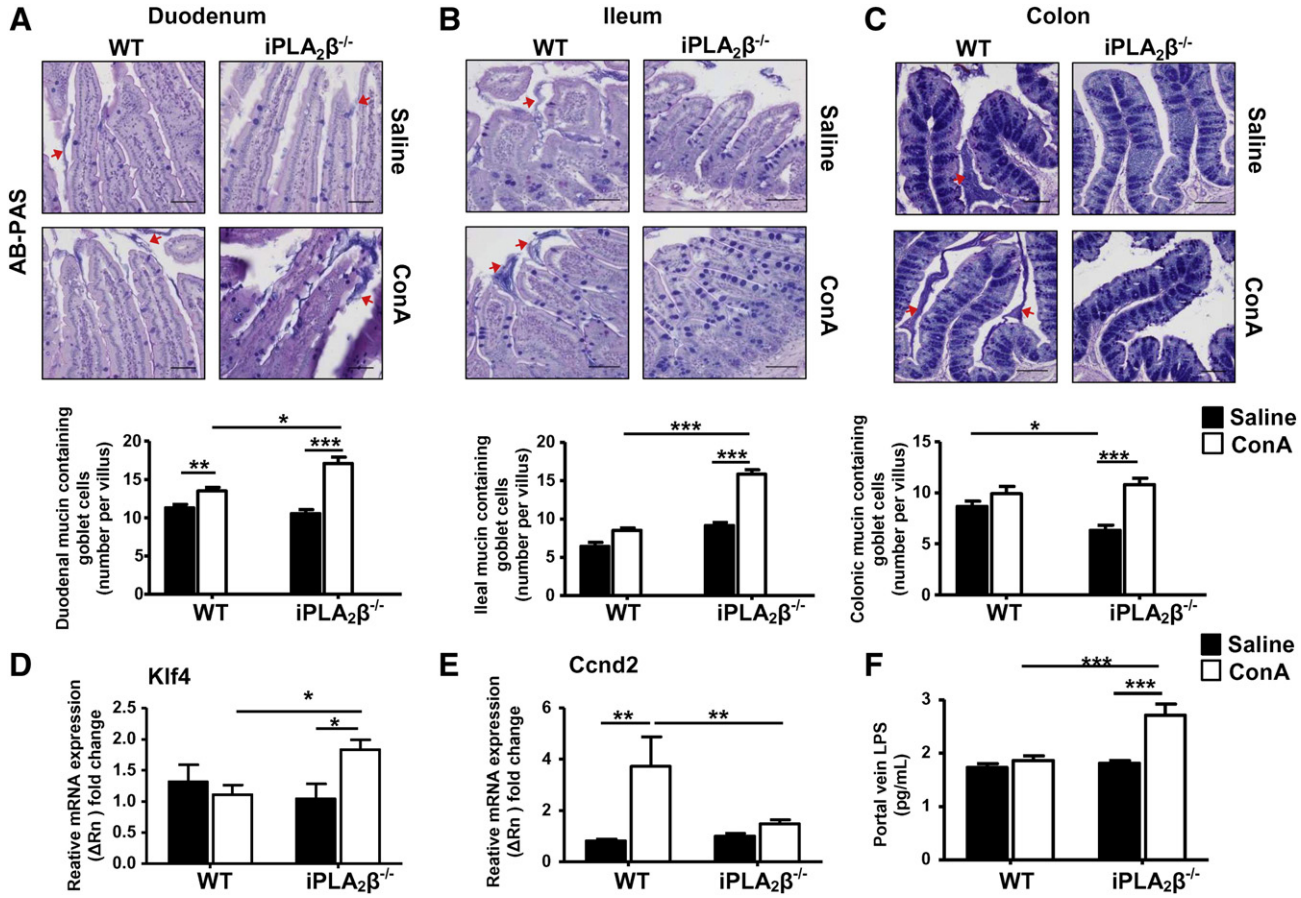

Fig. 4. iPLA$_2$β-deficient mice treated with ConA exhibit disrupted mucus membrane, goblet cell hyperplasia and endotoxin leakage to portal vein. Experimental conditions were the same as described in Fig. 1. A. Representative AB/PAS staining of the duodenum of treated mice from four groups showing goblet cells (upper panel), mucus secretion (indicated by arrow heads), and the quantification of mucin-containing duodenal goblet cell number (lower panel). Data are mean ± SEM (N = 3–4); *, $p < 0.05$; **, $p < 0.01$; ***, $p < 0.001$. B. Representative AB/PAS staining of the ileum of treated mice from four groups showing goblet cells (upper panel), mucus secretion (arrowheads), and the quantification of mucin-containing ileal goblet cell number (lower panel). Data are mean ± SEM (N = 3–4); ***, $p < 0.001$. C. Representative AB/PAS staining of the colon of treated mice from four groups showing goblet cells (upper panel), mucus secretion (arrowheads), and the quantification of mucin-containing colonic goblet cell number (lower panel). Data are mean ± SEM (N = 3–4); *, $p < 0.05$; ***, $p < 0.001$. D. qRT-PCR analysis of *Klf4* gene in the jejunum of treated mice from four groups. Data are mean ± SEM (N = 6–8); *, $p < 0.05$. E. qRT-PCR analysis of *Ccnd2* gene in the jejunum of treated mice from four groups. Data are mean ± SEM (N = 6–8); **, $p < 0.01$. F. ELISA analysis of LPS levels in portal vein serum. Data are mean ± SEM (N = 6–8); ***, $p < 0.001$. Scale bar in histological pictures represents 100 μm.

LCA. Active reabsorption of bile acids permits the return of bile acids to the liver via portal vein. In liver, 7-oxo-LCA is metabolized into CDCA and ursodeoxycholic acid (UDCA) by a steroid dehydrogenase. The metabolic loop through liver and gut constitutes an enterohepatic cycle of bile acids. In our experimental system, we utilized LC/MS-MS method to determine bile acid concentrations in liver, bile, intestine, feces, and peripheral serum (Table 1). By using the formula denoted in Table 1, the effects of iPLA$_2$β deficiency with and without ConA could be determined as indicated by an up- or down-arrow symbol, and the net change was represented as μg/g or μg/mL as well as % calculated based on total bile acids obtained from saline-treated WT mice.

In the liver, ConA treatment of WT mice caused marked elevation of most bile acids including the major bile acids in mice, namely CA, muriCA, and their conjugates (Table 1). However ConA treatment failed to elevate these bile acids in iPLA$_2$β$^{-/-}$ mice, and this resulted in a decrease in the response to ConA by iPLA$_2$β deficiency as indicated in the last column of Table 1. With an exception, rather than a decrease we observed a weak increase of hydrophobic bile acids CDCA + DCA and LCA. By combining the up and down response, a net decrease of liver bile acids was obtained with 1303 μg/g liver or 72%. This decrease in liver was consistently observed with a net decrease of bile acids in the bile by 689 μg/mL or 55%. We further determined whether bile acid synthesis genes were affected in the liver. We observed a significant decrease of Cyp7a1 mRNA expression when comparing ConA-treated WT with ConA-treated iPLA2β$^{-/-}$ livers (Fig. 5A), and the opposite was found for the expression of the negative regulator small heterodimer partner (SHP). Hence, iPLA$_2$β deficiency sensitized the effects of ConA by inhibiting bile acid synthesis in the liver.

We further performed RT-PCR analysis to determine whether bile acid transport genes were altered by ConA and iPLA2β deficiency. We observed a significant decreased mRNA expression of Ntcp and ABCB11/Bsep during ConA and iPLA$_2$β-deficiency sensitization (Fig. 5B). The decreased expression of Ntcp, which uptakes all conjugated bile acids from portal blood to hepatocytes, could at least in part contribute to the observed decreases of bile acids in the liver. Alternatively, the decreased expression of ABCB11/Bsep, which exports bile acids from hepatocytes into bile ducts, could in part contribute to the observed decreases of bile acids in the bile. ConA also caused a decrease in expression of phospholipid transport gene ABCB4 and MRP3 which exports bile acids from hepatocytes to portal blood, no difference was found among WT and mutant livers (Fig. 5B). No difference in liver FXR expression was observed among four treated groups (not shown).

Bile secreted from liver to gut lumen is mixed with fecal contents, and some bile acids are reabsorbed by intestinal cells. In a

Table 1
Conjugated and unconjugated bile acids in livers, bile, intestine, feces, and serum of iPLA$_2$β$^{-/-}$ and WT mice treated with saline or ConA.
Bile acids were detected by LC-MS/MS as described in Materials and methods. Results were expressed in μg/g tissue and μg/mL bile or serum, and represented as mean ± SEM (N = 6–11). Mice were treated with 10 mg/kg Con A or saline for 24 h.

Bile acid type[a]	Saline		Effect of iPLA$_2$β deficiency (μg/g or μg/mL)[a]	ConA		Response to ConA by iPLA$_2$β deficiency (μg/g or μg/mL)[b]
	WT	iPLA$_2$β$^{-/-}$		WT	iPLA$_2$β$^{-/-}$	
Liver						
CA	35.3 ± 15.4	305.3 ± 145.2	↑270	142.0 ± 49.4†	248.4 ± 144.1	↓164
muriCA	576.9 ± 86.6	263.8 ± 50.8*	↑313	942.6 ± 220.1	182.0 ± 52.5	↓448
tauroCA	527.4 ± 151.2	399.8 ± 162.3	↓128	999.8 ± 420.9†	545.9 ± 216.0#	↓326
tauromuriCA	504.4 ± 110.	576.9 ± 83.0	↑73	671.4 ± 165.7	456.8 ± 70.2	↓287
CDCA + DCA	0.09 ± 0.02	0.38 ± 0.05*	↑0.3	0.12 ± 0.03	0.42 ± 0.08#	↑0.01
glycoCDCA + glycoDCA	0.019 ± 0.006	0.042 ± 0.010	↓0.02	0.012 ± 0.006	0.024 ± 0.016	↓0.01
tauroCDCA + tauroDCA	135.7 ± 43.9	120.7 ± 38.5	↓15	169.1 ± 78.2	103.2 ± 30.5	↓51
LCA	0.014 ± 0.011	0.100 ± 0.006	↑0.09	0.023 ± 0.019	0.154 ± 0.112#	↑0.05
tauroLCA	0.40 ± 0.04	0.63 ± 0.15	↑0.2	0.62 ± 0.07	0.81 ± 0.15	↓0.04
UDCA	0.09 ± 0.04	0.38 ± 0.18	↑0.3	0.7 ± 0.44	0.89 ± 0.90	↓0.1
tauroUDCA	20.9 ± 6.9	38.1 ± 19.8	↑17	32.9 ± 18.3	22.3 ± 8.25	↓28
Net change in μg/g (% based on total 1801 μg/g liver WT/sal)			↓95 (↓5%)			↓1303 (↓72%)
Bile						
CA	217.7 ± 50.8	236.6 ± 88.3	↑19	122.8 ± 25.7	111.5 ± 30.9	↓30
muriCA	133.0 ± 36.5	147.8 ± 58.9	↑15	88.7 ± 16.4	69.6 ± 18.9	↓34
tauroCA	1.2 ± 0.1	1.3 ± 0.2	↑0.1	1.8 ± 0.1	0.8 ± 0.1#	↓1.1
tauromuriCA	6.2 ± 0.9	6.0 ± 1.4	↓0.2	8.0 ± 0.6	3.6 ± 0.6#	↓4.2
glycoCA	2.6 ± 0.5	2.9 ± 0.5	↑0.3	4.1 ± 0.4	2.2 ± 0.4#	↓2.2
CDCA + DCA	19.6 ± 2 5.4	24.0 ± 3 3.2	↑4.4	18.2 ± 3.1	19.3 ± 2.9	↓3.3
glycoCDCA + glycoDCA	91.9 ± 19.0	100.4 ± 27.7§	↑8.5	89.2 ± 6.6	22.8 ± 4.6#	↓75
tauroCDCA + tauroDCA	293.6 ± 37.5	289.0 ± 60.2§	↓4.6	348.1 ± 21.8	126.4 ± 34.2#	↓217
UDCA	47.9 ± 15.4	50.2 ± 13.0	↑2.3	39.1 ± 4.2	54.5 ± 9.3	↑13
tauroLCA	1.1 ± 0.2	1.4 ± 0.4§	↑0.3	1.1 ± 0.1	0.3 ± 0.1#	↓0.5
tauroUDCA	216.9 ± 39.0	214.6 ± 43.2	↓2.3	258.3 ± 22.7	124.6 ± 28.5#	↓131
glycoUDCA	231.6 ± 43.7	254.3 ± 61.0	↑23	344.9 ± 50.3	164.3 ± 33.2#	↓203
Net change in μg/mL (%based on total 1263 μg/mL bile WT/sal)			↑65 (↑5%)			↓689 (↓55%)
Intestine						
CA	209.6 ± 33.4	209.2 ± 40.1	↑0.2	155.9 ± 45.2	94.1 ± 23.0	↓58
muriCA	241.0 ± 62.9	100.1 ± 26.8	↓82	178.7 ± 63.8	23.6 ± 16.6#	↓73
tauroCA	57.9 ± 14.1	2.4 ± 0.8*	↓56	2.0 ± 0.6	1.2 ± 0.4	↑55
tauromuriCA	38.7 ± 12.4	2.0 ± 0.6*	↓37	2.8 ± 1.6	1.0 ± 0.3	↑35
glycoCA	0.85 ± 0.20	0.04 ± 0.01*	↓0.8	0.02 ± 0.01	0.01 ± 0.003	↑0.8
glycomuriCA	0.28 ± 0.08	0.03 ± 0.01*	↓0.3	0.006 ± 0.002	0.001 ± 0.0004	↑0.3
CDCA + DCA	4.09 ± 1.36	1.69 ± 0.29*	↓2	3.10 ± 0.90	0.54 ± 0.07#	↓0.2
glycoCDCA + glycoDCA	0.029 ± 0.009	0.003 ± 0.001*	↓0.03	0.002 ± 0.001†	0.0003 ± 0.0001	↑0.02
tauroCDCA + tauroDCA	19.82 ± 4.23	0.37 ± 0.10*	↓20	0.31 ± 0.09†	0.15 ± 0.03	↑19
LCA	0.14 ± 0.03	0.04 ± 0.009*	↓0.1	0.029 ± 0.009†	0.017 ± 0.004	↑0.1
tauroLCA	0.30 ± 0.006	0.04 ± 0.006*	↓0.3	0.03 ± 0.01†	0.005 ± 0.002	↑0.2
UDCA	7.56 ± 1.56	3.84 ± 0.85	↓4	7.63 ± 2.53	1.13 ± 0.30#	↓3
tauroUDCA	76.04 ± 20.22	3.48 ± 1.39*	↑73	1.02 ± 0.40†	0.77 ± 0.22	↑72
glycoUDCA	0.069 ± 0.027	0.0048 ± 0.0023*	↓0.06	0.0086 ± 0.0036†	0.017 ± 0.008	↑0.1
Net change in μg/g (% based on total 650 μg/g intestine WT/sal)			↓333 (↓51%)			↑48 (↑7%)
Feces						
CA	8.8 ± 3.1	24.1 ± 6.8	↑15	29.2 ± 11.3	39.3 ± 18.1	↓5
muriCA	85.8 ± 6.3	86.6 ± 11.6	↑0.8	105.4 ± 15.2	131.9 ± 29.6	↑26
tauroCA	0.13 ± 0.06	0.41 ± 0.22*§	↑0.3	0.24 ± 0.06	0.11 ± 0.01	↓0.4
tauromuriCA	0.4 ± 0.1	1.4 ± 0.4	↑1.0	0.7 ± 0.1	1.6 ± 0.5	↓0.1
glycoCA	0.10 ± 0.04	0.40 ± 0.21	↑0.3	0.56 ± 0.33	1.07 ± 0.59	↑0.2
CDCA + DCA	12.2 ± 1.4	12.5 ± 1.8	↑0.3	21.2 ± 3.1	10.7 ± 0.9#	↓11
glycoCDCA + glycoDCA	0.47 ± 0.10	0.37 ± 0.09	↓0.1	0.53 ± 0.08	0.19 ± 0.04	↓0.2
tauroCDCA + tauroDCA	0.44 ± 0.12	1.01 ± 0.36	↑0.6	0.61 ± 0.15	1.00 ± 0.39	↓0.2
LCA	4.3 ± 0.4	4.7 ± 0.8§	↑0.4	3.7 ± 0.4	1.7 ± 0.1#	↓2
Net change in μg/g (% based on total 113 μg/g feces WT/sal)			↑19 (↑17%)			↑6.6 (↑5.8%)
Serum						
CA	0.73 ± 0.4	1.4 ± 0.4	↑0.7	0.68 ± 0.06	1.69 ± 0.46	↑0.34
muriCA	0.76 ± 0.11	0.49 ± 0.1	↓0.3	0.83 ± 0.1	4.4 ± 0.7#	↑3.8
tauroCA	0.81 ± 0.2	0.06 ± 0.1§	↓0.8	0.24 ± 0.08	5.81 ± 0.5#	↑6.3
tauromuriCA	0.58 ± 0.14	0.29 ± 0.12§	↓0.3	0.43 ± 0.14	3.43 ± 0.88#	↑3.2
glycoCA	0.003 ± 0.002	0.0007 ± 0.0005§	↓0.02	0.002 ± 0.001	0.184 ± 0.007#	↑0.2
CDCA + DCA	0.07 ± 0.02	0.07 ± 0.02§	–	0.04 ± 0.01	0.87 ± 0.27#	↑0.8
tauroCDCA + tauroDCA	0.08 ± 0.01	0.05 ± 0.02	↓0.03	0.06 ± 0.03	3.92 ± 1.33	↑4
LCA	0.29 ± 0.011	0.50 ± 0.006§	↑0.2	0.56 ± 0.019	1.21 ± 0.112	↑0.4
UDCA	0.09 ± 0.02	0.10 ± 0.02	↑0.01	0.07 ± 0.01	0.44 ± 0.09*	↑0.4

(continued on next page)

Table 1 (*continued*)

Bile acid type[a]	Saline		Effect of iPLA$_2$β deficiency (μg/g or μg/mL)[a]	ConA		Response to ConA by iPLA$_2$β deficiency (μg/g or μg/mL)[b]
	WT	iPLA$_2$β$^{-/-}$		WT	iPLA$_2$β$^{-/-}$	
tauroUDCA	0.02 ± 0.004	0.02 ± 0.002	–	0.02 ± 0.005	0.60 ± 0.22[#]	↑0.4
Net change in μg/mL (%based on total 3.4 μg/mL serum WT/sal)			↓0.5 (↓13%)			↑20 (↑590%)

* $p < 0.05$, saline-WT versus saline-iPLA$_2$β$^{-/-}$.
\# $p < 0.05$, ConA-WT versus ConA-iPLA$_2$β$^{-/-}$.
§ $p < 0.05$, ConA-iPLA$_2$β$^{-/-}$ versus saline-iPLA$_2$β$^{-/-}$.
† $p < 0.05$, ConA-WT versus saline-WT.
[a] Response to ConA by iPLA$_2$β deficiency in μg/g or μg/mL = Mean $_{\text{Saline-iPLA2β}-/-}$ − Mean $_{\text{Saline-WT}}$.
[b] Response to ConA by iPLA$_2$β deficiency in μg/g or μg/mL = (Mean $_{\text{ConA-iPLA2β-/-}}$ − Mean $_{\text{Saline-iPLA2β-/-}}$) − (Mean $_{\text{ConA-WT}}$ − Mean $_{\text{Saline-WT}}$).

similar manner as liver and bile, the levels of major unconjugated bile acids CA and muriCA were decreased in the intestine in response to ConA by iPLA$_2$β deficiency; while most conjugated bile acids were increased (Table 1). This resulted in a net increase of bile acids by 48 μg/g or 7%. This net increase of bile acids may reflect specific changes in bile acid transports, thus we further measured expression of intestinal bile acid transport genes as well as farnesoid X-activated receptor (FXR). FXR is the major regulator of negative feedback loop that controls bile acid synthesis in the liver via an intestinal induction and release of fibroblast growth factor 15 (FGF15) into portal vein [34]. FGF15 in blood interacts with FGFR4-Klotho complex at the hepatocyte plasma membrane

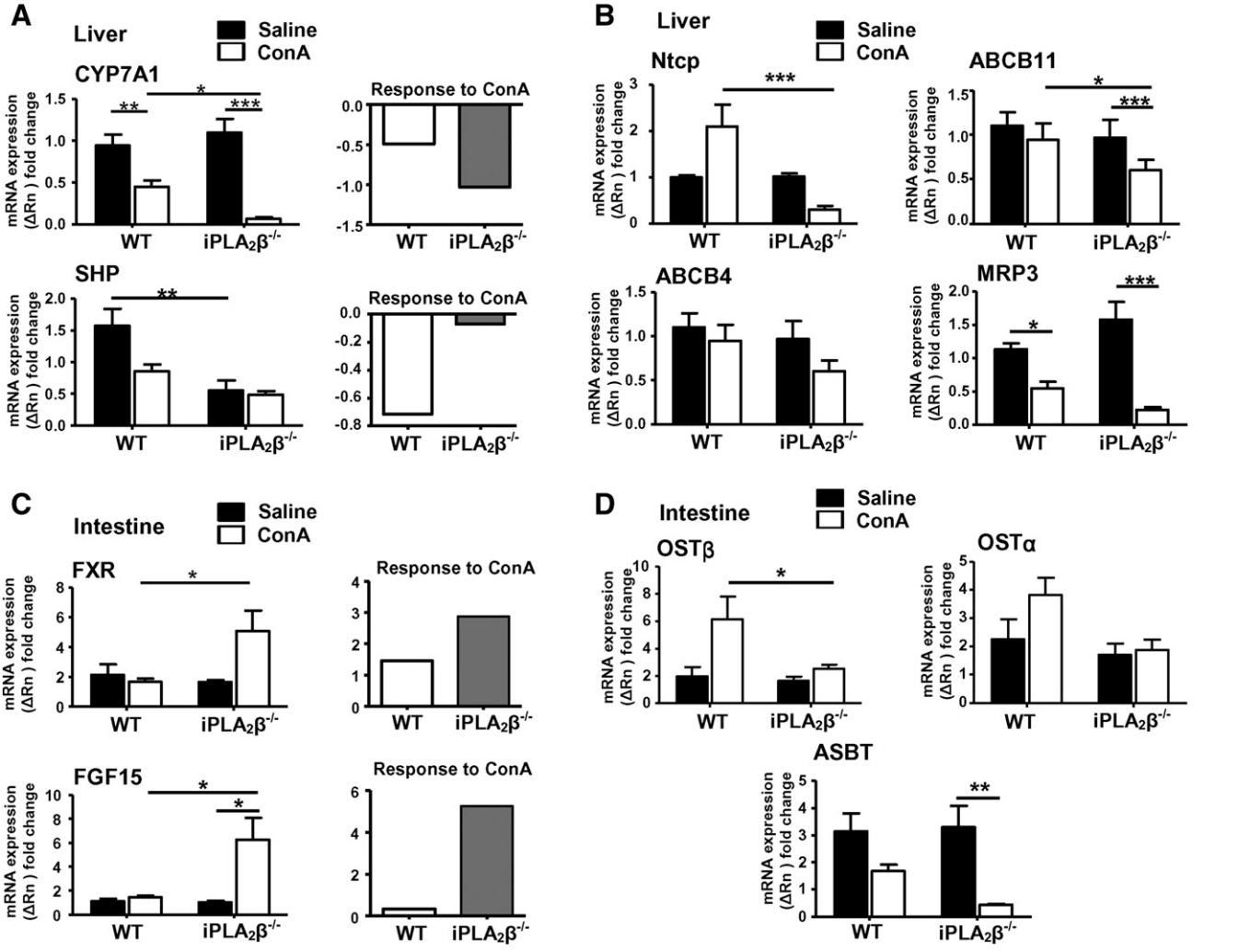

Fig. 5. iPLA$_2$β deficiency in response to ConA causes alteration in regulators of bile acid synthesis and bile acid transporters. Experimental conditions were the same as described in Fig. 1. A. qRT-PCR analysis of CYP7A1, and SHP mRNA expression in livers of treated mice from four groups (left panel), and the response to ConA was compared among WT (white bar) and iPLA$_2$β$^{-/-}$ (gray bar) mice (right panel). B. qRT-PCR analysis of Ntcp, ABCB11, ABCB4, and MRP3 mRNA expression in livers of treated mice from four groups. C. qRT-PCR analysis of FGF15, and FXR mRNA expression in the jejunum of treated mice from four groups (left panel), and the response to ConA was compared among WT (white bar) and iPLA$_2$β$^{-/-}$ (gray bar) mice (right panel). D. qRT-PCR analysis of intestinal OSTα, OSTβ, and ASBT mRNA expression in the jejunum of treated mice from four groups. Data are mean ± SEM (N = 4−7); *, $p < 0.05$, **, $p < 0.01$, ***, $p < 0.001$. The response to ConA in gene expression was calculated based on the formula: (Mean $_{\text{ConA/iPLA}_2\text{β}-/-}$-Mean $_{\text{Saline/iPLA}_2\text{β}-/-}$) for iPLA$_2$β$^{-/-}$ mice, and (Mean $_{\text{ConA/WT}}$ − Mean $_{\text{Saline/WT}}$) for WT mice.

triggering signaling cascade that represses Cyp7a1 mRNA expression, and hence bile acid synthesis in liver. Here, we observed that ConA sensitization by iPLA$_2$β deficiency was associated with a significant increase in intestinal FXR and FGF15 mRNA expression (Fig. 5C). We surmise that intestinal FGF15 could repress Cyp7a1 expression in the liver (Fig. 5A) hence resulting in the observed decreased bile acids in liver and bile (Table 1).

As for bile acid levels in feces, we observed a net increase of mainly muriCA of 6.6 μg/g or 5.8% during ConA and iPLA$_2$β-deficiency sensitization. This weak increase rather than the expected decrease as seen in the bile could be due to a multiple-fold dilution of bile acids from bile into a much larger volume of the whole feces. We further determined possible alteration of bile acids transports in the intestine. In response to ConA by iPLA$_2$β deficiency, we observed a significant decreased mRNA expression of OSTβ and only a tendency of a decrease for OSTα, and ASBT expression. OSTβ exports bile acids from enterocytes to portal blood thus its decreased expression could lead to an intestinal accumulation of bile acids.

As we demonstrated an increase of portal vein LPS in ConA-treated iPLA$_2$β-null mice (Fig. 4F), this provided a hint of a loss of intestinal barrier associated with duodenal atrophy where intestinal bile acids may leak into mesentery blood and subsequently into peripheral blood. In line with this, we observed a net increase of bile acids in peripheral blood from inferior vena cava by 20 μg/mL or 590%. Because that the net decreases of bile acids in liver and bile could not explain this increase in peripheral blood, we surmise that the loss of intestinal barrier rather than damaged bile ducts would likely contribute to the bile acids leaking outside the enterohepatic loop.

Finally, we also observed changes in bile acid profiles by iPLA$_2$β deficiency alone with a net decrease in the liver, and intestine by 5%, and 51%, respectively, and a mild increase in bile and feces of 5% and 17%, respectively (Table 1). These changes were associated with a significant decrease of SHP mRNA expression when comparing saline-treated WT with saline-treated iPLA$_2\beta^{-/-}$ livers (Fig. 5A). Thus, iPLA$_2$β deficiency alone appeared to have no overt abnormalities in terms of bile acid metabolism consistent with no marked pathology observed in liver and intestine of mutant mice (Figs. 1 and 2).

4. Discussion

We clearly demonstrated that iPLA$_2$β deficiency elicited sensitization towards ConA-induced AIH by causing hepatobiliary injury with increased releases of liver enzymes, apoptosis, lymphocyte infiltration, hepatic fibrosis, and ductular biliary expansion. This sensitization led to intestinal villous atrophy, inflammation, and goblet cell hyperplasia with more prominent effects observed in the duodenum than in the distal intestine. This sensitization was associated with increased portal vein LPS, suppressed levels of hepatic and biliary bile acids, but with marked increases of bile acids in peripheral blood. The latter was likely due to the loss of intestinal barrier and decreased bile acid transport into hepatocytes as a result of suppressed hepatic Ntcp expression. Hence, iPLA$_2$β deficiency may represent a genetic susceptibility precondition for AIH which leads to intestinal abnormalities resembling enteropathy. Our data further demonstrated the regulation of hepatic bile acid synthesis by intestinal FXR/FGF15 axis during AIH sensitization by iPLA$_2$β deficiency.

The mechanism of how iPLA$_2$β deficiency renders susceptibility for liver injury has been a subject in an on-going work in our laboratory which is based on a link between accumulated apoptosis and development of inflammation and autoimmune disease [35]. We found that livers of iPLA$_2\beta^{-/-}$ mice had increased apoptosis [24] with a moderate lymphocyte infiltration (Fig. 1F), and that Kupffer cells isolated from mutant mice secrete increased IFNγ and TNFα upon LPS stimulation (unpublished data). Upon ConA treatment of iPLA$_2\beta^{-/-}$ mice, liver lymphocytes (activated by ConA) together with Kupffer cells (activated by iPLA$_2$β deficiency) could augment the releases of cytokines thereby aggravating liver injury. Kupffer cells are known to play an important role in ConA-induced AIH by an activation of the production of reactive oxygen species [36] and CCL3 [37], both of which can induce innate immune activation [38]. Being proximal to the liver, the duodenum was the most affected by iPLA$_2$β deficiency and ConA sensitization, while inflammation was increased in jejunum, and goblet cell hyperplasia was observed in duodenum and ileum. It is plausible that activated Kupffer cells and liver lymphocytes during this sensitized AIH may release pro-inflammatory cytokines into intestinal tract which may in turn activate intestinal macrophages which cause the observed abnormalities. This is supported by a recent observation showing that activated macrophages with IL-6 release disrupt intestinal barrier function in the duodenum of patients with cirrhosis [9]. In line with this, the jejunum of ConA-treated mutant mice showed increased innate response cytokines CD14, TNFα, IL-6, and SOCS3, some of which contribute to IBD [39]. Activation of CCL3/CCR5 axis was also observed associated with intestinal atrophy in ConA-treated mutant mice, and this may be crucial in colitis-associated fibroblast accumulation [40] and IBD [41]. Furthermore, mucus secreted by intestinal goblet cells is critically involved in protection of intestinal mucosa as a physical and chemical barrier preventing adherence of microbiota and translocation of potential pathogens. Severely disturbed mucus membrane observed in the duodenum of ConA-treated mutant mice would allow the translocation of microbial toxins and endotoxin into intestinal mucosa, and into portal vein. The portal vein LPS may reach the liver and aggravate further inflammation there.

Our work shed light on the functions of intestinal FXR and FGF15 on their putative role as a metabolic regulator of bile acid synthesis in the liver [34]. AIH sensitization by iPLA$_2$β deficiency was associated with an upregulation of intestinal FXR/FGF15 and downregulation of hepatic Cyp7A1 expression, and the latter showing inhibited bile acid synthesis was supported by the observed decreases of hepatic and biliary bile acids by 55–72%. This occurred despite of the fact that we had observed an increase in biliary ductular reaction detected by CK19 staining. Under this condition, the expression of major bile acid transporters, such as hepatic Ntcp, ABCB11/Bsep, and intestinal OSTβ, was also markedly inhibited likely due to cytokines which were elevated in both organs [42]. Suppressed Ntcp would result in an accumulation of bile acids in portal vein, and this could be an additional mechanism for elevated bile acids in periphery blood. Notably, despite of the decreases of most bile acids in liver, the contents of CDCA + DCA and LCA in the liver were increased either by iPLA$_2$β deficiency alone or combined with ConA, and this was associated with decreased SHP expression. These conditions may indicate an inherent predisposition and toxic effects of these hydrophobic bile acids [13], seen as lymphocyte infiltration and mild ductular reaction in mutant livers.

In light of the reported anti-inflammatory effects of bile acids [43], the observed decreases of hepatic and biliary bile acids may augment the AIH injury sensitized by iPLA$_2$β deficiency. This can be further supported by reports that cholic acid administration results in a delay in the progression of acetaminophen-induced in liver injury [44], and a bile acid as an FXR receptor sensor protects against ConA-induced AIH [45]. During AIH injury sensitized by iPLA$_2$β deficiency, we observed an upregulation of intestinal FXR/FGF15 mRNA concomitant with an increase of most conjugated bile acids in the intestine. This intestine-specific activation, particularly by conjugated bile acids [46] may serve as a protective mechanism in protecting mice from overt cholestasis [47], and from gut barrier dysfunction [48] under this AIH sensitization. In line with this notion, intestinal bile acids are thought to act as an adaptation to reduce liver injury and cirrhosis [49]. Further experiments are warranted to test this hypothesis by co-administration with cholate or an FXR agonist to determine their protective effects against sensitized AIH. Furthermore, the defect of microbiota function in fecal bile acid metabolism has been shown to play a role in cirrhosis [14] and IBD [50]. In the feces of ConA-treated mutant mice, we observed an increase of muriCA while most secondary bile acids including LCA were decreased. This was suggestive of a defect in bacterial activity in the

dehydroxytion of muriCA to LCA [51]. Furthermore, the observed increases of bile acids in intestine and feces may evoke mucin secretion [52] resulting in the observed goblet cell hyperplasia.

We unequivocally demonstrated bile acid leakage into peripheral blood which was associated with duodenal atrophy and leakage of endotoxin into portal vein. Our interpretation for the impaired intestinal barrier as a mechanism for leaky bile acids in peripheral blood is supported by various clinical studies in that the serum contents of bile acids are elevated in children with hepatic and intestinal diseases [53], and in patients with IBD [54]. Much earlier work in the 1980's fails to show an association between liver disease and severe IBD, where no marked changes were seen in portal vein bile acids [55]. This contradiction to our study could be due to the fact that we used a much improved LC-MS/MS method for bile acid detection. In the 1990's, it was already shown that the contents of bile acids in duodenal juice from infants with hepatitis were significantly lower [56], which is in line with the observed decreases of hepatic and biliary bile acids in ConA-sensitized mutant mice. While our experimental model emphasizing iPLA$_2\beta$ as the genetic background for susceptibility for autoimmune disease, our results are consistent with reported clinical studies in susceptible individuals, e.g., infants with hepatitis and cholestasis [56], and an autoimmune adult with chronic hepatitis suffering from diarrhea with mucus, and abdominal pain [57].

In conclusion, AIH induced by ConA could be could be sensitized by a genetic background with iPLA$_2\beta$ deficiency, which leads to an induction of duodenal apoptosis, villous atrophy, bowel inflammation and goblet hyperplasia. Bile acid profiling revealed a defect in hepatic bile acid synthesis which was regulated by intestinal FXR/FGF15 axis. The observed increase of peripheral bile acids in our study could be used as a diagnostic marker for intestinal damage during sensitized AIH. Our data are consistent with clinical studies linking AIH to IBD [3], and it may be worthwhile to investigate whether these patients would have a defect in Pla2G6 gene as previously found in patients with neuroregenerative dystrophy [58]. Our study emphasizes that the liver-to-gut axis injury does exist during AIH in susceptible hosts.

Supplementary data to this article can be found online at http://dx.doi.org/10.1016/j.bbadis.2015.04.025.

Transparency document

The Transparency document associated with this article can be found in online version.

Acknowledgements

We thank Dr. John Turk who provided us with iPLA$_2\beta$-null mice and genotyping method used in our study. This study was supported by Deutsche Forschungsgemeinschaft grants (CH 288/6-1 and STR 216/15-3). We thank Dr. Jiliang Wang for his assistance in setting up the AIH model, and Dr. Bahador Javaheri for assistance in IHC techniques.

References

[1] M.P. Manns, A. Vogel, Autoimmune hepatitis, from mechanisms to therapy, Hepatology 43 (2006) S132–S144.
[2] R. Saich, R. Chapman, Primary sclerosing cholangitis, autoimmune hepatitis and overlap syndromes in inflammatory bowel disease, World J. Gastroenterol. 14 (2008) 331–337.
[3] R. Perdigoto, H.A. Carpenter, A.J. Czaja, Frequency and significance of chronic ulcerative colitis in severe corticosteroid-treated autoimmune hepatitis, J. Hepatol. 14 (1992) 325–331.
[4] A.A. Abdo, V.G. Bain, K. Kichian, S.S. Lee, Evolution of autoimmune hepatitis to primary sclerosing cholangitis: A sequential syndrome, Hepatology 36 (2002) 1393–1399.
[5] J. Hong-Curtis, M.M. Yeh, D. Jain, J.H. Lee, Rapid progression of autoimmune hepatitis in the background of primary sclerosing cholangitis, J. Clin. Gastroenterol. 38 (2004) 906–909.
[6] A.J. Czaja, Cholestatic phenotypes of autoimmune hepatitis, Clin. Gastroenterol. Hepatol. 12 (2014) 1430–1438.
[7] A.F. Hofmann, The continuing importance of bile acids in liver and intestinal disease, Arch. Intern. Med. 159 (1999) 2647–2658.
[8] A. Ramachandran, R. Prabhu, S. Thomas, J.B. Reddy, A. Pulimood, K.A. Balasubramanian, Intestinal mucosal alterations in experimental cirrhosis in the rat: role of oxygen free radicals, Hepatology 35 (2002) 622–629.
[9] J.Du. Plessis, H. Vanheel, C.E. Janssen, L. Roos, T. Slavik, P.I. Stivaktas, M. Nieuwoudt, S.G. van Wyk, W. Vieira, E. Pretorius, M. Beukes, R. Farré, J. Tack, W. Laleman, J. Fevery, F. Nevens, T. Roskams, S.W. Van der Merwe, Activated intestinal macrophages in patients with cirrhosis release NO and IL-6 that may disrupt intestinal barrier function, J. Hepatol. 58 (2013) 1125–1132.
[10] G. Kakiyama, P.B. Hylemon, H. Zhou, W.M. Pandak, D.M. Heuman, D.J. Kang, H. Takei, H. Nittono, J.M. Ridlon, M. Fuchs, E.C. Gurley, Y. Wang, R. Liu, A.J. Sanyal, P.M. Gillevet, J.S. Bajaj, Colonic inflammation and secondary bile acids in alcoholic cirrhosis, Am. J. Physiol. Gastrointest. Liver Physiol. 306 (2014) G929–G937.
[11] G. Tiegs, J. Hentschel, A. Wendel, A T cell-dependent. Experimental liver injury in mice inducible by concanavalin A, J. Clin. Invest. 90 (1992) 196–203.
[12] D. Chen, R.J. McKallip, A. Zeytun, Y. Do, C. Lombard, J.L. Robertson, T.W. Mak, P.S. Nagarkatti, M. Nagarkatti, CD44-deficient mice exhibit enhanced hepatitis after concanavalin A injection: evidence for involvement of CD44 in activation-induced cell death, J. Immunol. 166 (2001) 5889–5897.
[13] P. Fickert, A. Fuchsbichler, M. Wagner, G. Zollner, A. Kaser, H. Tilg, R. Krause, F. Lammert, C. Langner, K. Zatloukal, H.U. Marschall, H. Denk, M. Trauner, Regurgitation of bile acids from leaky bile ducts causes sclerosing cholangitis in Mdr2 (Abcb4) knockout mice, Gastroenterology 127 (2004) 261–274.
[14] J.M. Ridlon, J.M. Alves, P.B. Hylemon, J.S. Bajaj, Cirrhosis, bile acids and gut microbiota: unraveling a complex relationship, Gut Microbes 4 (2013) 382–387.
[15] S. Bao, H. Song, M. Wohltmann, S. Ramanadham, W. Jin, A. Bohrer, J. Turk, Insulin secretory responses and phospholipid composition of pancreatic islets from mice that do not express Group VIA phospholipase A2 and effects of metabolic stress on glucose homeostasis, J. Biol. Chem. 281 (2006) 20958–22073.
[16] J. Balsinde, M.A. Balboa, Cellular regulation and proposed biological functions of group VIA calcium-independent phospholipase A2 in activated cells, Cell. Signal. 17 (2005) 1052–1062.
[17] K. Lauber, E. Bohn, S.M. Kröber, Y.J. Xiao, S.G. Blumenthal, R.K. Lindemann, P. Marini, C. Wiedig, A. Zobywalski, S. Baksh, Y. Xu, I.B. Autenrieth, K. Schulze-Osthoff, C. Belka, G. Stuhler, S. Wesselborg, Apoptotic cells induce migration of phagocytes via caspase-3-mediated release of a lipid attraction signal, Cell 113 (2003) 717–730.
[18] R.B. Mueller, A. Sheriff, U.S. Gaipl, S. Wesselborg, K.B. Lauber, Attraction of phagocytes by apoptotic cells is mediated by lysophosphatidylcholine, Autoimmunity 40 (2007) 342–344.
[19] K.A. Carnevale, M.K. Cathcart, Calcium-independent phospholipase A(2) is required for human monocyte chemotaxis to monocyte chemoattractant protein 1, J. Immunol. 167 (2001) 3414–3421.
[20] R.S. Mishra, K.A. Carnevale, M.K. Cathcart, iPLA$_2\beta$: front and center in human monocyte chemotaxis to MCP-1, J. Exp. Med. 205 (2008) 347–359.
[21] X. Zhao, D. Wang, Z. Zhao, Y. Xiao, S. Sengupta, Y. Xiao, R. Zhang, K. Lauber, S. Wesselborg, L. Feng, T.M. Rose, Y. Shen, J. Zhang, G. Prestwich, Y. Xu, Caspase-3-dependent activation of calcium-independent phospholipase A2 enhances cell migration in non-apoptotic ovarian cancer cells, J. Biol. Chem. 281 (2006) 29357–29368.
[22] S. Ramanadham, K.E. Yarasheski, M.J. Silva, M. Wohltmann, D.V. Novack, B. Christiansen, X. Tu, S. Zhang, X. Lei, J. Turk, Age-related changes in bone morphology are accelerated in group VIA phospholipase A2 (iPLA2beta)-null mice, Am. J. Pathol. 172 (2008) 868–881.
[23] I. Malik, J. Turk, D.J. Mancuso, L. Montier, M. Wohltmann, D.F. Wozniak, R.E. Schmidt, R.W. Gross, P.T. Kotzbauer, Disrupted membrane homeostasis and accumulation of ubiquitinated proteins in a mouse model of infantile neuroaxonal dystrophy caused by PLA2G6 mutations, Am. J. Pathol. 172 (2008) 406–416.
[24] W. Xu, S. Tuma, N. Katava, A. Pathil-Warth, W. Strmmel, W. Chamulitrat, Deficiencies of Calcium-independent Phospholipase A2 B in vivo Causes Reduced Systemic Lipids and Lipoproteins Concomitant with Increased Hepatic Apoptosis and Inflammation, The International Liver CongressTM (EASL), Barcelona, Spain, April 18-22 2012.
[25] A.J. Czaja, Targeting apoptosis in autoimmune hepatitis, Dig. Dis. Sci. 59 (2014) 2890–2894.
[26] Y. Alnouti1, I.L. Csanaky, C.D. Klaassen, Quantitative-profiling of bile acids and their conjugates in mouse liver, bile, plasma, and urine using LC-MS/MS, J. Chromatogr. B Anal. Technol. Biomed. Life Sci. 873 (2008) 209–217.
[27] D. Haas, H. Gan-Schreier, C.-D. Langhans, T. Rohrer, G. Engelmann, M. Heverin, D.W. Russell, P.T. Clayton, G.F. Hoffmann, J.G. Okun, Differential diagnosis in patients with suspected bile acid synthesis defects, World J. Gastroenterol. 18 (2012) 1067–1076.
[28] A.K. Roshak, E.A. Capper, C. Stevenson, C. Eichman, L.A. Marshall, Human calcium-independent phospholipase A2 mediates lymphocyte proliferation, J. Biol. Chem. 275 (2000) 35692–35698.
[29] T.M. McIntyre, A.V. Pontsler, A.R. Silva, A. St Hilaire, Y. Xu, J.C. Hinshaw, G.A. Zimmerman, K. Hama, J. Aoki, H. Arai, G.D. Prestwich, Identification of an intracellular receptor for lysophosphatidic Acid (LPA): LPA is a transcellular PPARgamma agonist, Proc. Natl. Acad. Sci. U. S. A. 100 (2003) 131–136.
[30] K. Motojima, P. Passilly, J.M. Peters, F.J. Gonzalez, N. Latruffe, Expression of putative fatty acid transporter genes are regulated by peroxisome proliferator-activated receptor alpha and gamma activators in a tissue- and inducer-specific manner, J. Biol. Chem. 273 (1998) 16710–16714.
[31] M.E. Greenberg, M. Sun, R. Zhang, M. Febbraio, R. Silverstein, S.L. Hazen, Oxidized phosphatidylserine-CD36 interactions play an essential role in macrophage-dependent phagocytosis of apoptotic cells, J. Exp. Med. 203 (2006) 2613–2625.
[32] J.P. Katz, N. Perreault, B.G. Goldstein, C.S. Lee, P.A. Labosky, V.W. Yang, K.H. Kaestner, The zinc-finger transcription factor Klf4 is required for terminal differentiation of goblet cells in the colon, Development 129 (2002) 2619–2628.

[33] P.J. Real, V. Tosello, T. Palomero, M. Castillo, E. Hernando, E. de Stanchina, M.L. Sulis, K. Barnes, C. Sawai, I. Homminga, J. Meijerink, I. Aifantis, G. Basso, C. Cordon-Cardo, W. Ai, A. Ferrando, Gamma-secretase inhibitors reverse glucocorticoid resistance in T cell acute lymphoblastic leukemia, Nat. Med. 15 (2009) 50–58.
[34] C. Cicione, C. Degirolamo, A. Moschetta, Emerging role of fibroblast growth factors 15/19 and 21 as metabolic integrators in the liver, Hepatology 56 (2012) 2404–2411.
[35] L.E. Muñoz, K. Lauber, M. Schiller, A.A. Manfredi, M. Herrmann, The role of defective clearance of apoptotic cells in systemic autoimmunity, Nat. Rev. Rheumatol. 6 (2010) 280–289.
[36] H. Nakashima, M. Kinoshita, M. Nakashima, Y. Habu, S. Shono, T. Uchida, N. Shinomiya, S. Seki, Superoxide produced by Kupffer cells is an essential effector in concanavalin A-induced hepatitis in mice, Hepatology 48 (2008) 1979–1988.
[37] S. Okamoto, S. Yokohama, M. Yoneda, M. Haneda, K. Nakamura, Macrophage inflammatory protein-1alpha plays a crucial role in concanavalin A-induced liver injury through induction of proinflammatory cytokines in mice, Hepatol. Res. 32 (2005) 38–45.
[38] L. Chen, X.J. Xie, Y.F. Ye, L. Zhou, H.Y. Xie, Q.F. Xie, J. Tian, S.S. Zheng, Kupffer cells contribute to concanavalin A-induced hepatic injury through a Th1 but not Th17 type response-dependent pathway in mice, Hepatobiliary Pancreat. Dis. Int. 10 (2011) 171–178.
[39] A. Suzuki, T. Hanada, K. Mitsuyama, T. Yoshida, S. Kamizono, T. Hoshino, M. Kubo, A. Yamashita, M. Okabe, K. Takeda, S. Akira, S. Matsumoto, A. Toyonaga, M. Sata, A. Yoshimura, CIS3/SOCS3/SSI3 plays a negative regulatory role in STAT3 activation and intestinal inflammation, J. Exp. Med. 193 (2001) 471–481.
[40] S. Sasaki, T. Baba, K. Shinagawa, K. Matsushima, N. Mukaida, Crucial involvement of the CCL3-CCR5 axis-mediated fibroblast accumulation in colitis-associated carcinogenesis in mice, Int. J. Cancer 135 (2014) 1297–1306.
[41] S.L. Pender, V. Chance, C.V. Whiting, M. Buckley, M. EdwardsM, R. Pettipher, T.T. MacDonald, Systemic administration of the chemokine macrophage inflammatory protein 1alpha exacerbates inflammatory bowel disease in a mouse model, Gut 54 (2005) 1114–1120.
[42] R.M. Green, D. Beier, J.L. Gollan, Regulation of hepatocyte bile salt transporters by endotoxin and inflammatory cytokines in rodents, Gastroenterology 111 (1996) 193–198.
[43] J.W. Greve, D.,J. Gouma, W.A. Buurman, Bile acids inhibit endotoxin-induced release of tumor necrosis factor by monocytes: an in vitro study, Hepatology 10 (1989) 454–458.
[44] B. Bhushan, P. Borude, G. Edwards, C. Walesky, J. Cleveland, F. Li, X. Ma, U. Apte, Role of bile acids in liver injury and regeneration following acetaminophen overdose, Am. J. Pathol. 183 (2013) 1518–1526.
[45] A. Mencarelli, B. Renga, M. Migliorati, S. Cipriani, E. Distrutti, L. Santucci, S. Fiorucci, The bile acid sensor farnesoid X receptor is a modulator of liver immunity in a rodent model of acute hepatitis, J. Immunol. 183 (2009) 6657–6666.
[46] G.U. Denk, S. Maitz, R. Wimmer, C. Rust, P. Invernizzi, S. Ferdinandusse, W. Kulik, A. Fuchsbichler, P. Fickert, M. Trauner, A.F. Hofmann, U. Beuers, Conjugation is essential for the anticholestatic effect of NorUrsodeoxycholic acid in taurolithocholic acid-induced cholestasis in rat liver, Hepatology 52 (2010) 1758–1768.
[47] S. Modica, M. Petruzzelli, E. Bellafante, S. Murzilli, L. Salvatore, N. Celli, G. Di Tullio, G. Palasciano, T. Moustafa, E. Halilbasic, M. Trauner, A. Moschetta, Selective activation of nuclear bile acid receptor FXR in the intestine protects mice against cholestasis, Gastroenterology 142 (2012) 355–365.
[48] L. Verbeke, R. Farre, B. Verbinnen, K. Covens, T. Vanuytsel, J. Verhaegen, M. Komuta, T. Roskams, S. Chatterjee, P. Annaert, I.V. Elst, P. Windmolders, J. Trebicka, F. Nevens, W. Laleman, The FXR agonist obeticholic acid prevents gut barrier dysfunction and bacterial translocation in cholestatic rats, Am. J. Pathol. 185 (2015) 409–419.
[49] C.Y. Yeh, Y.W. Chung-Davidson, H. Wang, K. Li, W. Li, Intestinal synthesis and secretion of bile salts as an adaptation to developmental biliary atresia in the sea lamprey, Proc. Natl. Acad. Sci. U. S. A. 109 (2012) 11419–11424.
[50] H. Duboc, S. Rajca, D. Rainteau, D. Benarous, M.A. Maubert, E. Quervain, G. Thomas, V. Barbu, L. Humbert, G. Despras, C. Bridonneau, F. Dumetz, J.P. Grill, J. Masliah, L. Beaugerie, J. Cosnes, O. Chazouillères, R. Poupon, C. Wolf, J.M. Mallet, P. Langella, G. Trugnan, H. Sokol, P. Seksik, Connecting dysbiosis, bile-acid dysmetabolism and gut inflammation in inflammatory bowel diseases, Gut 62 (2013) 531–539.
[51] S.I. Sayin, A. Wahlström, J. Felin, S. Jäntti, H.U. Marschall, K. Bamberg, B. Angelin, T. Hyötyläinen, M. Orešič, F. Bäckhed, Gut microbiota regulates bile acid metabolism by reducing the levels of tauro-beta-muricholic acid, a naturally occurring FXR antagonist, Cell Metab. 17 (2013) 225–235.
[52] A. Barcelo, J. Claustre, F. Toumi, G. Burlet, J.A. Chayvialle, J.C. Cuber, P. Plaisancié, Effect of bile salts on colonic mucus secretion in isolated vascularly perfused rat colon, Dig. Dis. Sci. 46 (2001) 1223–1231.
[53] F. Kuipers, C.M. Bijleveld, C.M. Kneepkens, A. van Zanten, J. Fernandes, R.J. Vonk, Sulphated lithocholic acid conjugates in serum from children with hepatic and intestinal diseases, Scand. J. Gastroenterol. 20 (1985) 1255–1261.
[54] C. Gnewuch, G. Liebisch, T. Langmann, B. Dieplinger, T. Mueller, M. Haltmayer, H. Dieplinger, A. Zahn, W. Stremmel, G. Rogler, G. Schmitz, Serum bile acid profiling reflects enterohepatic detoxification state and intestinal barrier function in inflammatory bowel disease, World J. Gastroenterol. 15 (2009) 3134–3141.
[55] R.T. Holzbach, M.E. Marsh, M.R. Freedman, V.W. Fazio, I. Lavery, D.A. Jagelman, Portal vein bile acids in patients with severe inflammatory bowel disease, Gut 21 (1980) 428–435.
[56] H.Y. Hsu, S.Y. Tang, M.H. Chang, Analysis of duodenal bile acids by high performance liquid chromatography in infants with cholestasis, J. Formos. Med. Assoc. 90 (1991) 487–492.
[57] A. Carroccio, U. Volta, L. Di Prima, N. Petrolini, A.M. Florena, M.R. Averna, G. Montalto, A. Notarbartolo, Autoimmune enteropathy and colitis in an adult patient, Dig. Dis. Sci. 48 (2003) 1600–1606.
[58] A. Gregory, S.K. Westaway, I.E. Holm, P.T. Kotzbauer, P. Hogarth, S. Sonek, J.C. Coryell, T.M. Nguyen, N. Nardocci, G. Zorzi, D. Rodriguez, I. Desguerre, E. Bertini, A. Simonati, B. Levinson, C. Dias, C. Barbot, I. Carrilho, M. Santos, I. Malik, J. Gitschier, S.J. Hayflick, Neurodegeneration associated with genetic defects in phospholipase A(2), Neurology 71 (2008) 1402–1409.